HANOI UNIVERSITY OF SCIENCE AND TECHNOLOGY
SCHOOL OF ELECTRICAL AND ELECTRONIC ENGINEERING

PROJECT REPORT
DIGITAL CONTROL DESIGN

Topic: *Three – phase DC/AC Inverter*

Instructor: Asso.Prof. Vu Thi Thuy Nga

Student Name	Student's ID
Trịnh Hà Trang	20200630
Nguyễn Thế Anh	20200034
Nguyễn Bùi Thành An	20202730
Nguyễn Hoàng Minh	20207619

Ha Noi, 2024

TABLE OF CONTENTS

IMAGE INDEX

TABLE INDEX

CHAPTER 1. INTRODUCTION

1.1 DC/AC inverter

A DC-AC inverter is a device that converts direct current (DC) electricity into alternating current (AC) electricity. it takes power from a DC source, such as a battery or a solar panel, and transforms it into AC power that can be used to run appliances, electronic devices, or be fed into the electrical grid. The process involves changing the voltage level and waveform from the DC input to match the required characteristics of the AC output. The most common type of waveform for AC power is a sine wave, but some inverters may produce a modified sine wave or a square wave, which is generally suitable for simpler electronic devices.

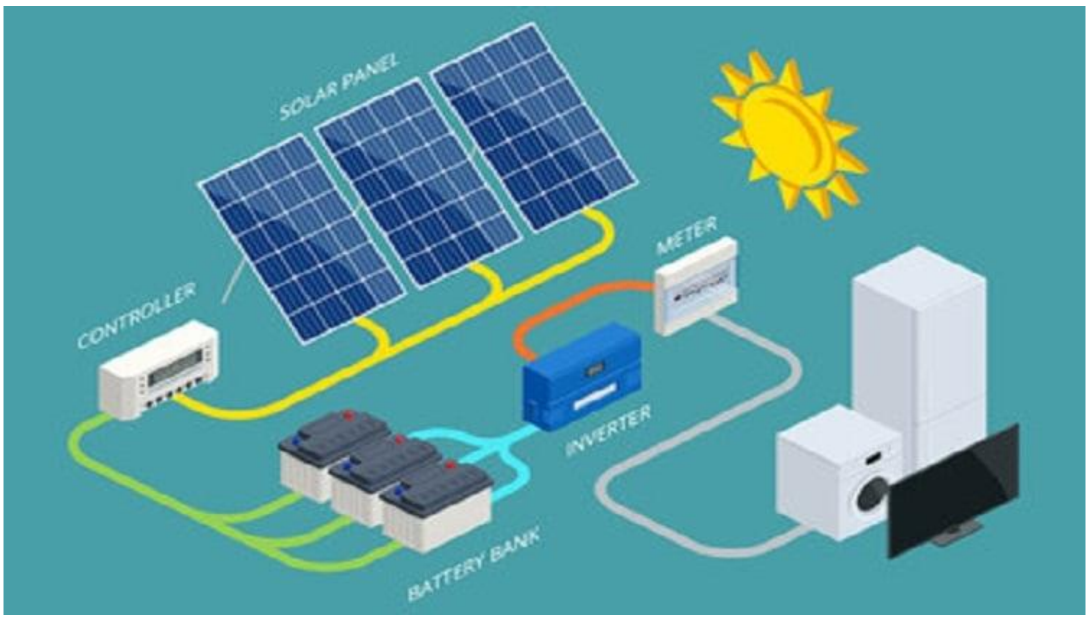

Figure 1. An example of an inverter application

When it comes to voltage source inverter(VSI) there are two common types: the single-phase and the three phase one. While the single-phase voltage source inverter (VSI) covers low-power applications, the three- phase VSI outperforms in the medium to high-power range, and the output of the three-phase VSI can be either synchronized with the grid voltage or only supply a residential load, depending on the applications and consumers power demand. There are two types of three-phase VSI: grid-tied and off-grid inverters, each of which is installed in a different circumstance and has different requirements. Off-grid three-phase VSI, which provide conditioned and uninterrupted power to critical loads such as telecommunication systems, data centers, airline computers, medical systems, and even an industrial site or a rural community when power outages occur by transferring backup energy stored in batteries, is widely used in Uninterruptible Power Supply (UPS) systems.

Furthermore, in recent years, both standby and grid-tied three-phase VSI have been seen being implemented in a Distributed Generation System (DGS) using renewable sources such as solar cells, fuel cells, wind turbines, biomass, and so on to relieve the burden on conventional grid utilities while meeting strict environmental requirements. When the DGS system is linked in parallel with the main grid, the three-phase VSI not only injects appropriate AC power into the grid, but it also contains features that deal with the islanding effect and provides grid inspection.

1.2 Structure & Working Principle

Figure 2 demonstrates the standard three-phase VSI structure. A three-phase VSI typically consists of two major components, the first of which is a DC voltage source. The DC voltage source can come from a storage bank such as a battery, a supercapacitor, or the output of a previous DC-DC converter. A DC-link capacitor after the input DC voltage source may be required in some cases to maintain a constant voltage across the inverter and protect it from voltage spikes, surges, and electromagnetic interference (EMI).

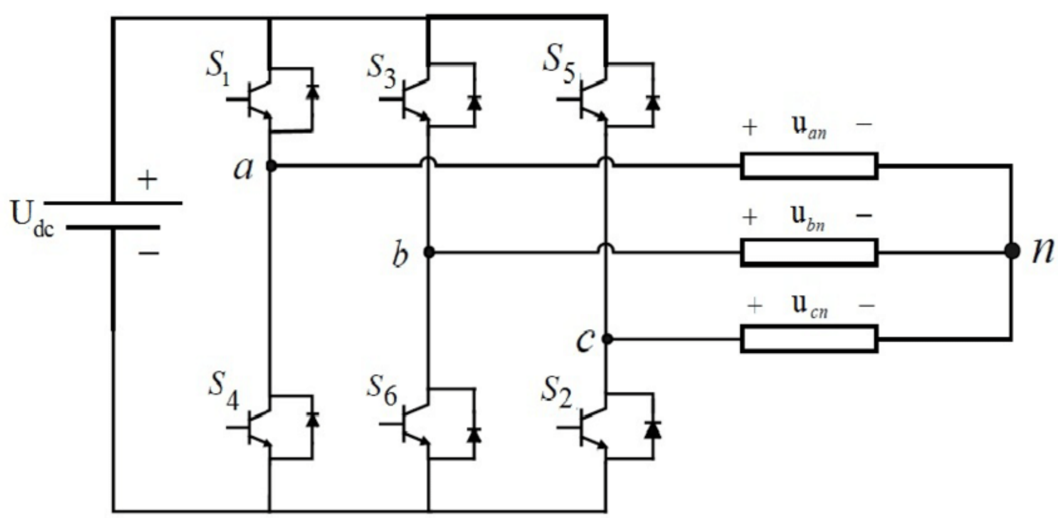

Figure *2. Standard 3-phase inverter*

Furthermore, the inverter is made up of six fully adjustable power switches that might be implemented with semiconductor devices such as GTOs, MOSFETs, or IGBTs. These devices are typically chosen depending on the switching frequency and power capacity requirements. Allowing the switches to conduct at the same time will result in a short circuit across the DC source. Similarly, the switches should not be turned off at the same time to avoid undefined output AC voltages and VSI states. In addition, when driving an inductive load, antiparallel diodes (or inverse-parallel diodes) must be added to provide reverse current routes to the source when the switch is turned off.

The correct output waveform of the three-phase inverter can be seen in Figure 3 below. In this figure the voltage is controlled by the SVPWM carrier signal. It is important to note that the waveform should be sine to optimally reduce harmonica and disturbances.

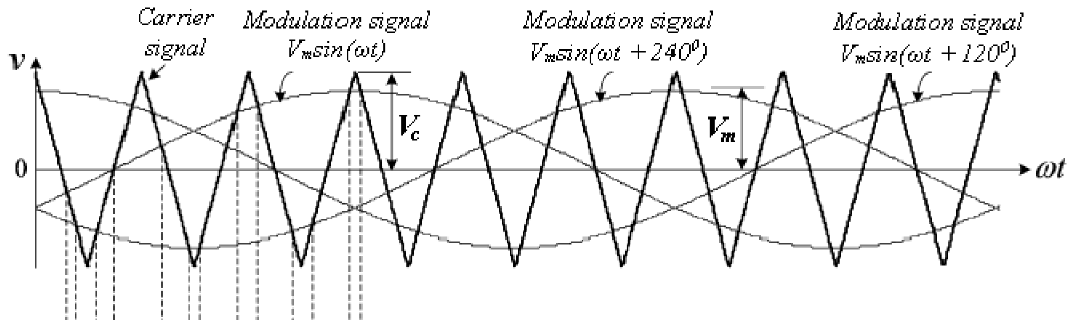

***Figure** 3. Ideal output waveform of the three-phase inverter*

1.3 Design Criteria

1.3.1. For inverter design

Rated power	48VA
Input DC voltage	24V
Output voltage	12V (RMS)
Output fundamental frequency	50Hz
Power factor	0.8
Maximum clock frequency	80MHz
Sensor	Voltage Sensor, Current Sensor

1.3.2. For controller design

- Expect no overshoot.
- Short settling time
- Low harmonic distortion
- Can work with different type of loads.

For this project we will only use resistance load.

CHAPTER 2. SYSTEM MODELING AND CONTROL DESIGN

2.1. Space Vector Pulse Width Modulation (SVPWM)

SVPWM is a modulation technique used to control the voltage applied to a three-phase electric motor, whether it is a permanent magnet or an induction machine. The purpose is to generate a three-phase sinusoidal waveform with adjustable frequency and amplitude using a constant DC voltage and six switches, such as transistors. To apply SVPWM, the Clark Transformation method must be employed.

2.1.1. Clark Transformation

Consider the three-phase voltage/current system $X = (X_a, X_b, X_c)$ and $X_a = X_b = X_c = 0$. By Clark transformation, it equals to a space vector:

$$\bar{u} = \frac{2}{3}(u_a + au_b + a^2u_c)$$

where $a = e^{j\frac{2\pi}{3}} = -\frac{1}{2} + j\frac{\sqrt{3}}{2}$

Express on alpha – beta axis:

$$\begin{cases} U_\alpha = \frac{1}{3}(2u_A - u_B - u_C) \\ U_\beta = \frac{1}{\sqrt{3}}(u_B - u_C) \end{cases}$$

Express by transformation matrix:

$$\begin{bmatrix} u_\alpha \\ u_\beta \end{bmatrix} = \frac{2}{3}\begin{bmatrix} 1 & -\frac{1}{2} & -\frac{1}{2} \\ 0 & \frac{\sqrt{3}}{2} & -\frac{\sqrt{3}}{2} \end{bmatrix}[u_A \quad u_B \quad u_C]$$

$$= T_1[u_A \quad u_B \quad u_C]$$

If $\begin{cases} u_A = U^m \cos(\omega t) \\ u_B = U^m \cos\left(\omega t - \frac{2\pi}{3}\right) \\ u_C = U^m \cos\left(\omega t + \frac{2\pi}{3}\right) \end{cases}$

Then $\bar{\boldsymbol{u}}$ is rotating vector:

$$\bar{u} = U^m e^{j(\omega t)}$$

2.1.2. Working principle of SVPWM

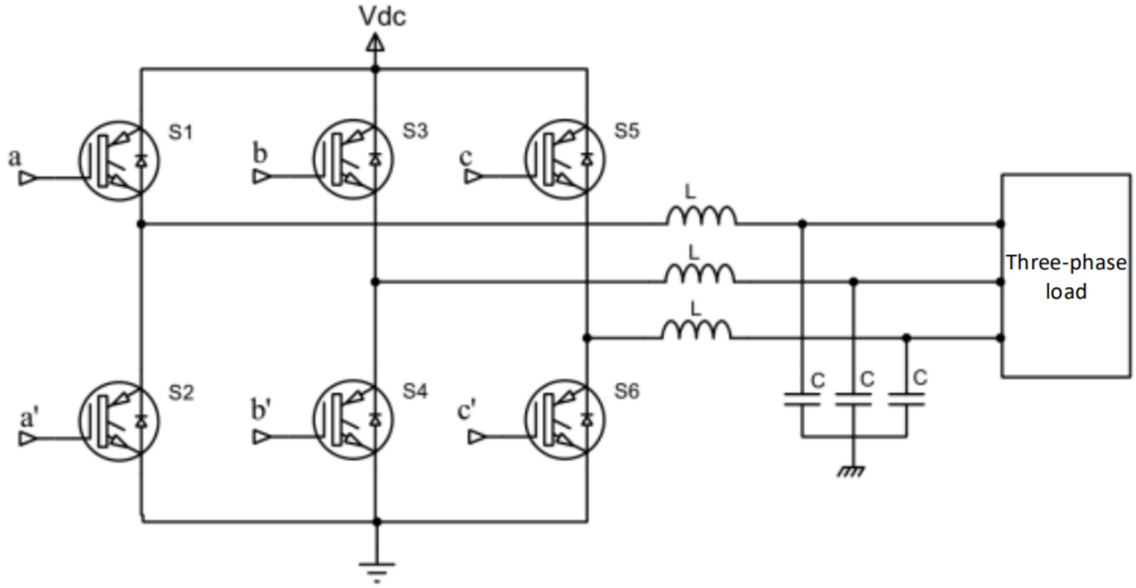

Figure 4. *Three phase voltage source PWM inverter*

The circuit model of a typical three-phase voltage source SVPWM inverter is shown in Fig. 4. S1 to S6 are the six power switches that shape the output, which are controlled by the switching variables a, a′, b, b′, c and c′. When an upper transistor is switched on, i.e., when a, b or c is 1, the corresponding lower transistor is switched off, i.e., the corresponding a′, b′ or c′ is 0. Therefore, the on and off states of the upper transistors S1, S3 and S5 can be used to determine the output voltage.

There are eight possible combinations of on and off patterns for the three upper power switches. The on and off states of the lower power devices are opposite to the upper one and so are easily determined once the states of the upper power transistors are determined. The relationship between the vector space and the corresponding switching states is shown in Table 1.

Table 1. Switching states and voltage values of the vectors

No	Turn-on switch	u_A	u_B	u_C	$\vec{V_s}$
U0	V2, V4, V6	0	0	0	0
U1	V6, V1, V2	$2/3U_{DC}$	$-1/3U_{DC}$	$-1/3U_{DC}$	$\frac{2}{3}U_{DC}e^{-j0}$
U2	V1, V2, V3	$1/3U_{DC}$	$1/3U_{DC}$	$-2/3U_{DC}$	$\frac{2}{3}U_{DC}e^{j\frac{\pi}{3}}$
U3	V2, V3, V4	$-1/3U_{DC}$	$2/3U_{DC}$	$-1/3U_{DC}$	$\frac{2}{3}U_{DC}e^{j\frac{2\pi}{3}}$
U4	V3, V4, V5	$-2/3U_{DC}$	$1/3U_{DC}$	$1/3U_{DC}$	$\frac{2}{3}U_{DC}e^{-j\pi}$
U5	V4, V5, V6	$-1/3U_{DC}$	$-1/3U_{DC}$	$2/3U_{DC}$	$\frac{2}{3}U_{DC}e^{-j\frac{2\pi}{3}}$
U6	V5, V6, V1	$1/3U_{DC}$	$-2/3U_{DC}$	$1/3U_{DC}$	$\frac{2}{3}U_{DC}e^{-j\frac{\pi}{3}}$
U7	V1, V3, V5	0	0	0	0

The space vector diagram is depicted in Fig 5.

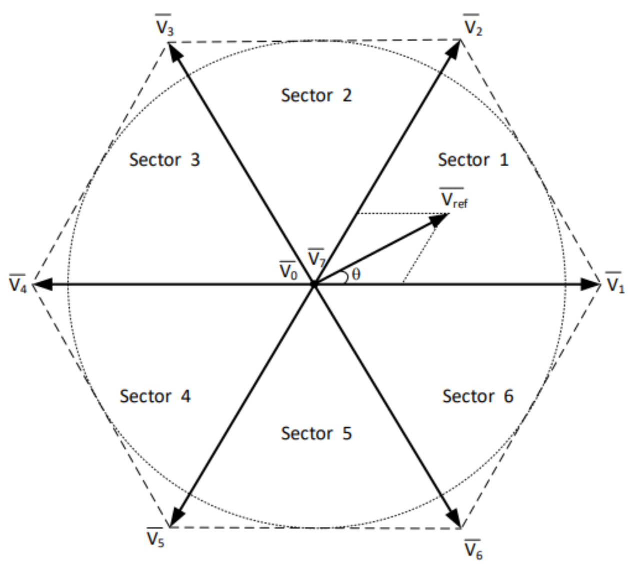

Figure 5. *Voltage Space Vectors*

To generate a sinusoidal three-phase voltage for the motor we have to construct a vector that rotates in plane space called the reference voltage vector $\overrightarrow{V_{ref}}$. The reference voltage vector rotates in space with angular velocity $\omega = 2\pi f$, where f is the fundamental frequency of the drive output voltage. As a result, when the reference voltage vector rotates one revolution in the space plane, the drive output changes one electrical cycle over time. The inverter's output frequency is equal to the rotation speed of the reference voltage vector.

The usual implementation of SVPWM involves the following steps:

(1) The coordinate transformation for the reference vector $\overrightarrow{V_{ref}}$. from a rotating frame to a stationary one.

(2) Define the time interval T1, T2, and T0.

(3) Determine the switching time of each Transistor (S1 - S6). The inverter cannot directly generate the desired reference voltage vector. The reference vector can be decomposed into two component vectors that lie on two other nonadjacent vectors and two zero vectors at the origin of the coordinate. Fig. 6 shows space vector PWM switching patterns at each sector.

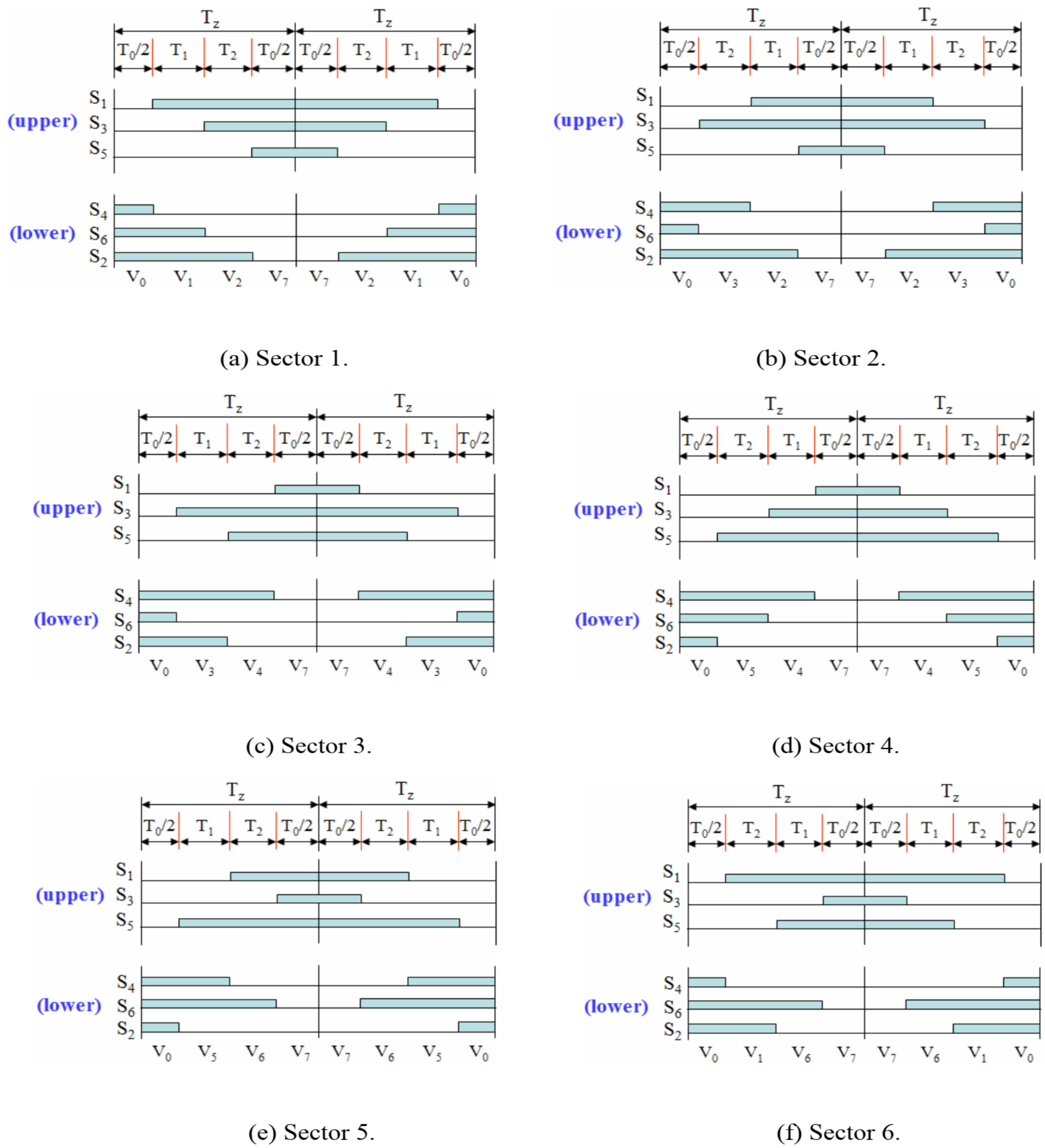

***Figure 6.** Space Vector PWM switching patterns at each sector*

2.2. Mathematical Modeling of Three – phase Inverter

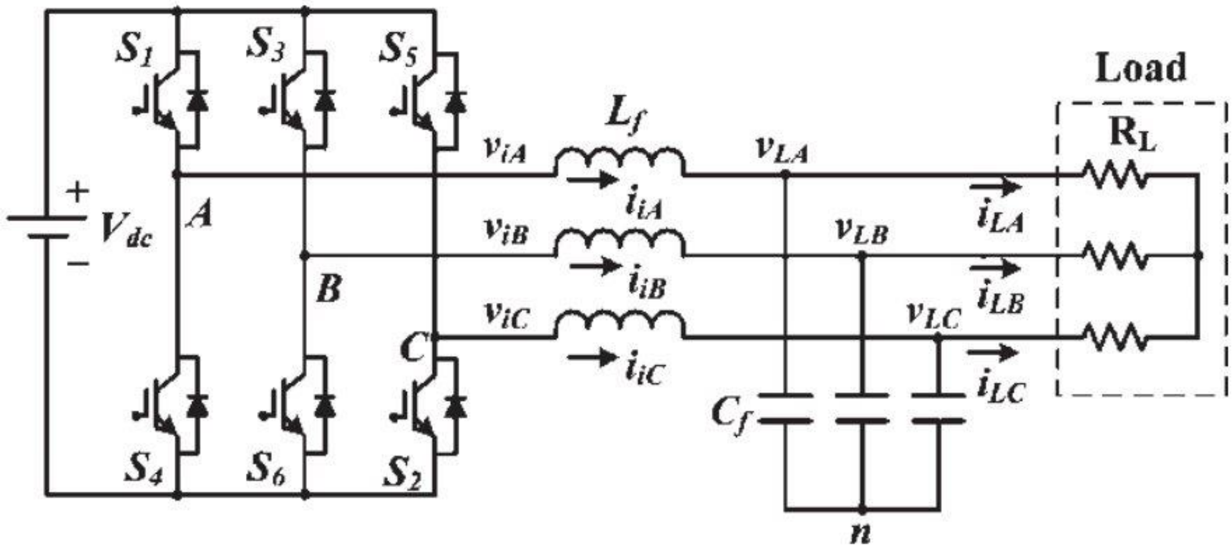

Figure 7. Schematic diagram of the three-phase inverter with resistance load

$V_i = [V_{iA}\ \ V_{iB}\ \ V_{iC}]^T$	Inverter output line to neutral voltage vector
$I_i = [I_{iA}\ \ I_{iB}\ \ I_{iC}]^T$	Inverter phase current vector
$V_L = [V_{LA}\ \ V_{LB}\ \ V_{LC}]^T$	Load line to neutral voltage vector
$I_L = [I_{LA}\ \ I_{LB}\ \ I_{LC}]^T$	Load phase current vector
$V_{id\text{-}q} = [V_{id}\ \ V_{iq}]^T$	*d-q* frame voltage vector of V_i
$I_{id\text{-}q} = [I_{id}\ \ I_{iq}]^T$	*d-q* frame current vector of I_i
$V_{Ld\text{-}q} = [V_{Ld}\ \ V_{Lq}]^T$	*d-q* frame voltage vector of V_L
$V_{i\alpha\text{-}\beta} = [V_{i\alpha}\ \ V_{i\beta}]^T$	*α-β* frame voltage vector of V_i
$I_{i\alpha\text{-}\beta} = [I_{i\alpha}\ \ I_{i\beta}]^T$	*α-β* frame current vector of I_i
$V_{L\alpha\text{-}\beta} = [V_{L\alpha}\ \ V_{L\beta}]^T$	*α-β* frame voltage vector of V_L

Fig. 7 illustrates a three-phase DC-AC inverter, incorporating an LC filter. The system includes a three-phase inverter (S1 to S6), output filters $(L_f\ and\ C_f)$, a three-phase resistive load (R_L), and a DC voltage source (V_{DC}). The LC filter is a critical component of this circuit, responsible for eliminating harmonic components of the inverter's output voltage resulting from high frequency switching actions.

Applying Kirchoff's Voltage Law and Kirchoff's Current Law at the output of the LC filter, we obtain:

$$\begin{cases} \frac{d\boldsymbol{V}_L}{dt} = \frac{1}{C_f}\boldsymbol{I}_i - \frac{1}{C_f}\boldsymbol{I}_L \\ \frac{d\boldsymbol{I}_i}{dt} + \frac{r_L}{L_f}\boldsymbol{I}_i = \frac{1}{L_f}\boldsymbol{V}_i - \frac{1}{L_f}\boldsymbol{V}_L \end{cases} \tag{1}$$

Clark Transformation:

$$\boldsymbol{X}_{\alpha\beta} = x_a e^{j0} + x_b e^{j\frac{2\pi}{3}} + x_c e^{j\frac{4\pi}{3}}$$

where $\boldsymbol{X_{\alpha\beta}} = x_\alpha + jx_\beta$

Eq. 1 can be transformed to the following:

$$\begin{cases} \frac{d\boldsymbol{V_{L\alpha\beta}}}{dt} = \frac{1}{C_f}\boldsymbol{I_{i\alpha\beta}} - \frac{1}{C_f}\boldsymbol{I_{L\alpha\beta}} \\ \frac{d\boldsymbol{I_{i\alpha\beta}}}{dt} + \frac{r_L}{L_f}\boldsymbol{I_{i\alpha\beta}} = \frac{1}{L_f}\boldsymbol{V_{i\alpha\beta}} - \frac{1}{L_f}\boldsymbol{V_{L\alpha\beta}} \end{cases} \tag{2}$$

Park Transformation:

$$\boldsymbol{X_{dq}} = x_d + jx_q = \boldsymbol{X_{\alpha\beta}} e^{-j\theta}$$

where $\theta(t) = \int_0^t \omega(\tau)d\tau + \theta_o$ is the transformation angle, ω is the angular frequency ($\omega = 2\pi f$)

Eq. 2 can be transformed to the following:

$$\begin{cases} \frac{d\boldsymbol{V_{Ldq}}}{dt} + j\omega\boldsymbol{V_{Ldq}} = \frac{1}{C_f}\boldsymbol{I_{idq}} - \frac{1}{C_f}\boldsymbol{I_{Ldq}} \\ \frac{d\boldsymbol{I_{idq}}}{dt} + \frac{r_L}{L_f}\boldsymbol{I_{idq}} + j\omega\boldsymbol{I_{Ldq}} = \frac{1}{L_f}\boldsymbol{V_{idq}} - \frac{1}{L_f}\boldsymbol{V_{Ldq}} \end{cases} \tag{3}$$

Eq. 3 can be expressed as:

$$\begin{cases} \dot{v}_{Ld} = \omega v_{Lq} - \frac{1}{C_f} i_{Ld} + \frac{1}{C_f} i_{id} & (4) \\ \dot{v}_{Lq} = -\omega v_{Ld} - \frac{1}{C_f} i_{Lq} + \frac{1}{C_f} i_{iq} & (5) \\ \dot{\iota}_{id} + \frac{r_L}{L_f} i_{id} = -\frac{1}{L_f} v_{Ld} + \omega i_{iq} + \frac{1}{L_f} v_{id} & (6) \\ \dot{\iota}_{iq} + \frac{r_L}{L_f} i_{iq} = -\frac{1}{L_f} v_{Lq} - \omega i_{id} + \frac{1}{L_f} v_{iq} & (7) \end{cases}$$

2.3. Control design

The block diagram of the three – phase inverter control is shown in Fig 9.

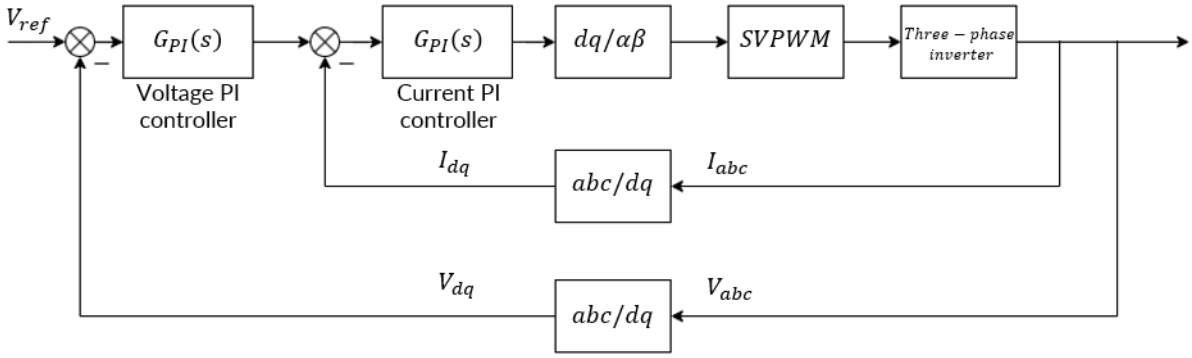

Figure 8. *Block diagram of the three - phase inverter control*

To approach the digital control of this system, we decided to first design the system in continuous domain, find the parameters for the continuous PI controllers and from that, approximate to find the parameters for the discrete PI controllers. The transfer function of PI controller is:

$$G_{PI}(s) = K_P\left(1 + \frac{1}{T_i s}\right) \tag{8}$$

A two-loop design is considered in this project, with the outer loop is the voltage loop which uses the output voltage as feedback, while the inner loop is the current loop. The design sequence is to first starts with the current loop, then the voltage loop. Note that since the two-loop is designed in dq frame, there exists a cross-coupling between d and q-axis components in both loops, which reduces the overall dynamic and steady-state of the system. It is essential to use decoupling methods to avoid the mentioned phenomena.

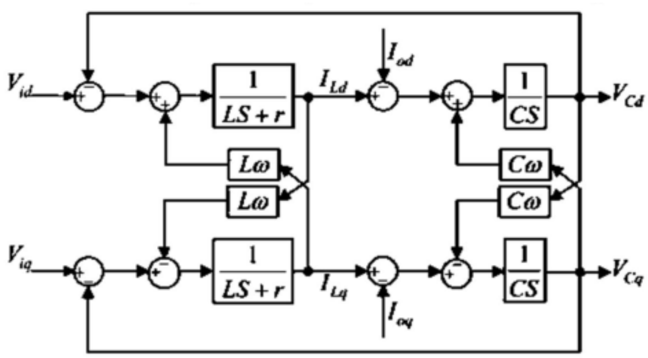

Figure 9*. Decoupling methodology for three – phase inverter modeling in dq frame*

2.3.1. Inner current control loop

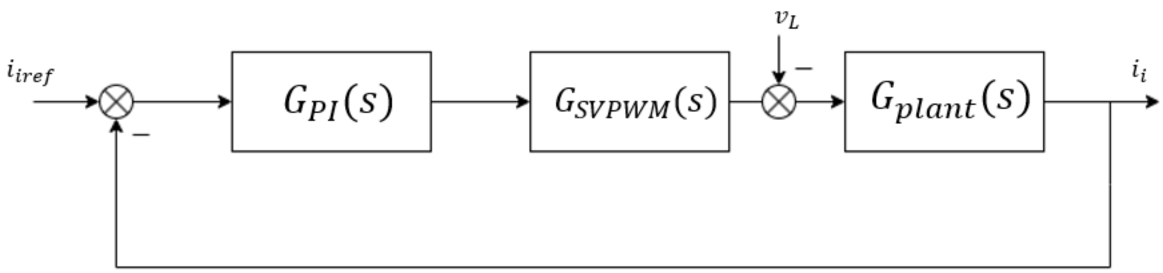

Figure 10. *Block diagram of the current control loop*

From (6), (7), we have

$$\begin{cases} L_f \frac{dv_{id}}{dt} + r_L i_{id} = -v_{Ld} + L_f \omega i_{iq} + v_{id} \\ L_f \frac{v_{iq}}{dt} + r_L i_{iq} = -v_{Lq} - L_f \omega i_{id} + v_{iq} \end{cases} \quad (9)$$

It is clearly seen in Eq. (9) that the injected AC current can be controlled by regulating the output voltage of the DC/AC converter. However, the d- and q- axis output currents are coupled to each other, leading to a slightly complicated system from the control perspective. In addition, the load voltage also has an influence on the control dynamics. Therefore, the output voltage references (i.e., $v_{id,ref}$ and $v_{iq,ref}$) are modified by means of adding one decoupling term and one feed-forward voltage as

$$\begin{cases} v_{id,ref} = -v_{Ld} + \omega L_f i_{iq} + v_{id} \\ v_{iq,ref} = -v_{Lq} - \omega L_f i_{id} + v_{iq} \end{cases} \quad (10)$$

The current control loop after modification can be rewritten as

$$\begin{cases} L_f \frac{di_{id}}{dt} + r_L i_{id} = v_{id,ref} \\ L_f \frac{di_{iq}}{dt} + r_L i_{iq} = v_{iq,ref} \end{cases} \quad (11)$$

in which the d- and q-axis output currents (i.e., the current injected to the load) are decoupled, as shown in Fig. 4. Moreover, as it is shown in Eq. 11, the d- and q-axis output current expressions are identical. Thus, the analysis on one axis is sufficient, as they share the same dynamics. Accordingly, the plant transfer functions from the converter output voltage references to the output current currents can be obtained as

$$G_{plant} = \frac{I_i(s)}{V_i(s)} = \frac{1}{r_L + L_f s} = \frac{1}{r_L\left(1 + \frac{L_f}{r_L} s\right)} \quad (12)$$

The Space vector PVM transfer function $\left(G_{SVPWM}(s)\right)$:

$$G_{SVPWM}(s) = e^{-\frac{T_S}{2}s} = \frac{1}{1+\frac{T_S}{2}s} \tag{13}$$

As shown in Fig. 10, the transfer function of the current regulator is

$$G(s) = G_{PWM}(s).G_{Plant}(s) = \frac{1}{r_L\left(1+\frac{L_f}{r_L}s\right)} \times \frac{1}{1+\frac{T_S}{2}s} = \frac{k}{(1+T_1 s)(1+T_2 s)} \tag{14}$$

where $T_2 = \frac{T_S}{2} = 10^{-4}; T_1 = \frac{L_f}{r_L} = 0.5,\ k = \frac{1}{r_L} = \frac{5000}{33}$

As can be seen that, the Eq. 14 is the second – order system, which has $T_1 \gg T_2$. Therefore, magnitude optimum method is applied in this controller (Eq. 15)

$$\begin{cases} K_P = \frac{T_1}{2kT_2} \\ T_i = T_1 \end{cases} \tag{15}$$

The parameter of the current PI controller will be $\begin{cases} K_P = 16.5 \\ T_i = 0.5 \end{cases} \Longrightarrow \begin{cases} K_P = 16.5 \\ K_i = 33 \end{cases}$ (16)

Fig. 11 and Fig. 12 below shows the simulation and result of the current control loop

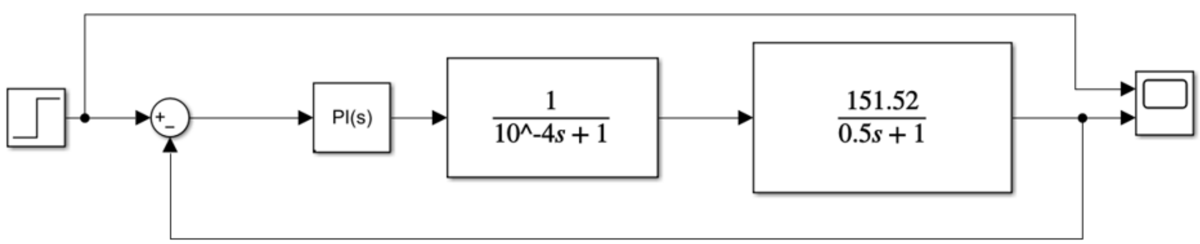

Figure 11. *Simulation of current control loop*

Figure 12. *Simulation result of current control loop*

2.3.2. Outer voltage control loop

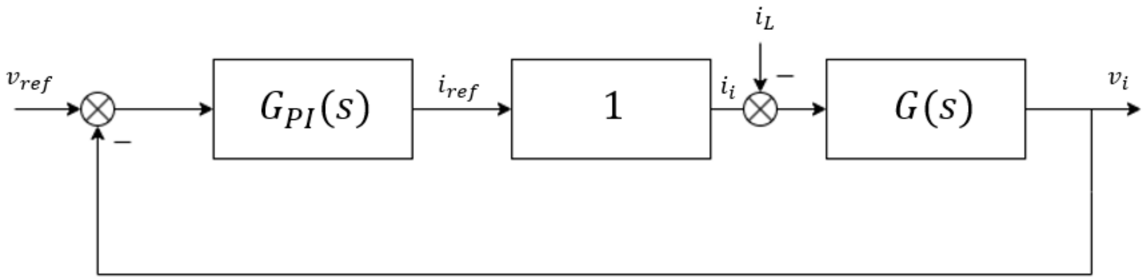

Figure 13. Block diagram of the voltage control loop

The response of current loop is much more faster than the voltage loop, so the transfer function of current is considered 1 (Fig. 12). From (6), (7), we have

$$\begin{cases} C_f \dfrac{dv_{Ld}}{dt} = C_f \omega v_{Lq} - i_{Ld} + i_{id} \\ C_f \dfrac{dv_{Lq}}{dt} = -C_f \omega v_{Ld} - i_{Lq} + i_{iq} \end{cases} \tag{17}$$

Similar to the current control loop, decoupling method is also applied in the voltage control loop. Thus, the transfer function of the voltage regulator can be written as

$$G(s) = \frac{V_{id}(s)}{I_{id}(s)} = \frac{V_{iq}(s)}{I_{iq}\ (s)} = \frac{1}{sC_f} \tag{18}$$

For choosing parameter K_P, K_I of the PI controller of voltage loop, MATLAB tunning is considered. We decided to choose $\begin{cases} K_P = 0.09 \\ K_I = 20.8 \end{cases}$ (19)

Fig. 14 and Fig. 15 below shows the simulation and result of the voltage control loop

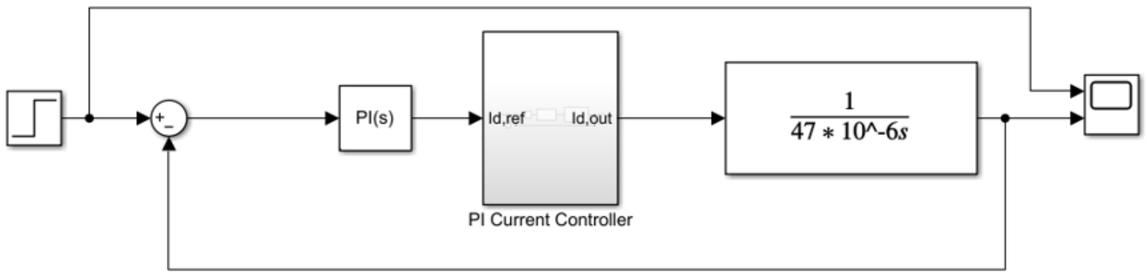

Figure 14. Simulation of voltage control loop

Figure 15. Simulation result of voltage control loop

2.3.3. PI controller in Z – domain

The general equation of the digital PI controller: $u(t) = u_P(t) + u_I(t)$

+) Proportional: $u_P(k) = K_P e(k)$

+) Integral: $u_I(k) = u_I(k-1) + \frac{T}{T_i} e(k)$

$$\Longrightarrow u(k) = K_P e(k) + u_I(k-1) + \frac{T}{T_i} e(k) \tag{20}$$

We have: $u(k-1) = u_P(k-1) + u_I(k-1) \Longrightarrow u_I(k-1) = u(k-1) - K_P e(k-1)$

From Eq. (20):

$$u(k) = K_P e(k) + u(k-1) - K_P e(k-1) + \frac{T}{T_i} e(k) \tag{21}$$

$$\Longrightarrow u(k) = u(k-1) + \left(K_P + \frac{T}{T_i}\right) e(k) - e(k-1) K_p \tag{22}$$

CHAPTER 3. HARDWARE SETUP

3.1. System specification

Table 2. System specification of three – phase DC/AC Inverter

Input Voltage (VDC)	**24**V DC
Output Voltage (VOUT)	**12**V AC
Output fundamental frequency (f)	**50**Hz
Output Power (Load Power) (POUT)	**8**W
Switching frequency(fSW)	**5**kHz

3.2. Block Diagram

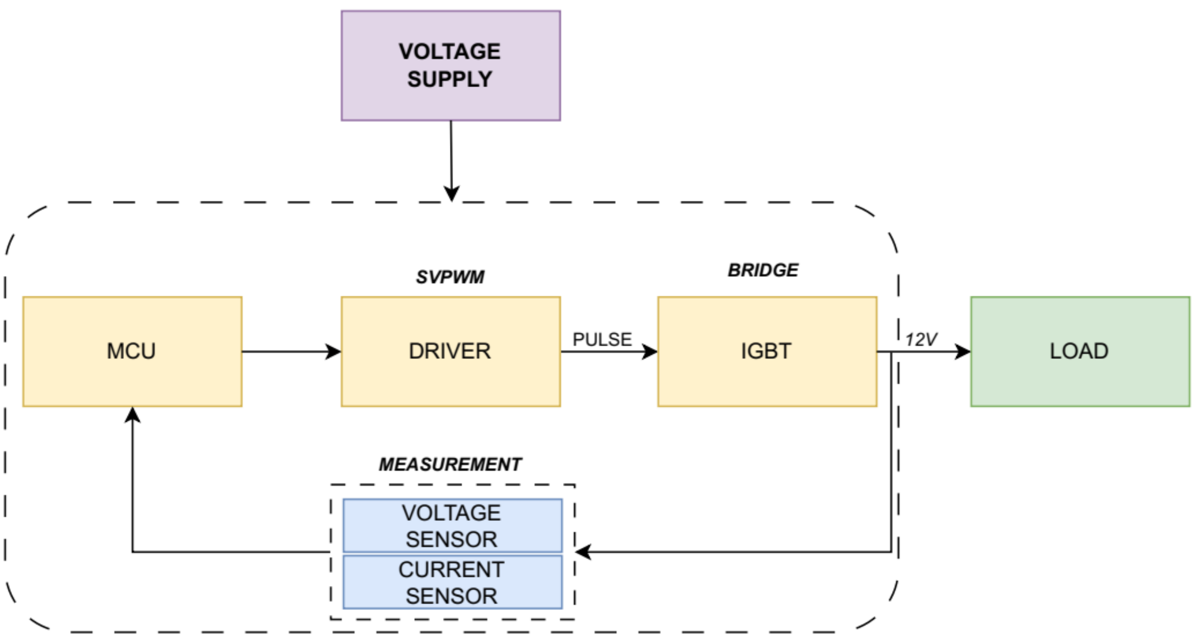

Figure 16. The block diagram of system

3.3. Calculation and Solution for components

3.3.1. Input for inverter (DC Voltage)

Normally, the drop voltage on the inductor in output filter equals to 10% $Vout$ the input DC voltage, so the minimum of required DC Voltage can be calculated as following:

$$V_{DC\_min} = 1,1 * \frac{\sqrt{2}*\mathrm{V_{out}}}{0,9} = 1,1 * \frac{\sqrt{2}*12}{0,9} = 21\ (V)$$

⇒ Choose V_{in} = 24(V)

⇒ Choosing Adaptor convert AC 220V to 24V

Figure 17. *Adaptor convert 220V~AC to 24V*

3.3.2. Output Current

Maximum current value: $I_{out\ max} = \sqrt{2} * \frac{S_{out}}{\sqrt{3}*V_{OUT}*} = \sqrt{2} * \frac{30}{3*\frac{12}{\sqrt{3}}} = 2(A)$

3.3.3. IGBTs and Diode

With a power factor cos(σ) = 0,8, the avarage current flowing through IGBT is:

$$I_{avg} = \frac{1}{2\pi}\int_{\varphi}^{\pi} I_{out_{max}} \sin(\theta - \varphi) * d\theta = \frac{1 + cos\varphi}{2\pi} * I_{out_{max}} = \frac{1 + 0,8}{2\pi} * 2 = 0,57(A)$$

The avarage current flowing through antiparrallel diodes is:

$$I_{avg} = \frac{1}{2\pi}\int_{0}^{\varphi} I_{out_{max}} \sin(\theta - \varphi) * d\theta = \frac{1 - cos\varphi}{2\pi} * I_{out_{max}} = \frac{1 - 0,8}{2\pi} * 2 = 0,06(A)$$

⇒ Choosing IGBT IRF840 MOSFET

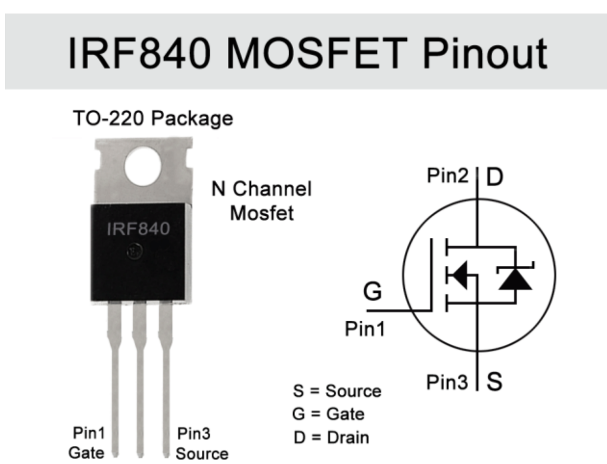

⇒

⇒ ***Figure 18*** *.RF840 And Pin diagram*

Table 3. *Parameter of IRF840 MOSFET*

Property	Value	Unit	Description
Type	MOSFET (N-Channel)		
Continuous Drain Current (ID)	8	A	Maximum current the IGBT can handle continuously at 25°C case temperature.
Drain-Source Voltage (VDS)	500	V	Maximum voltage that can be applied between drain and source terminals.
Gate-Source Voltage (VGS)	±20	V	Maximum voltage that can be applied between gate and source terminals.
Threshold Voltage (VGS(th))	4	V	Voltage at which the IGBT starts to conduct current.
On-Resistance (RDS(on))	0.85	Ω	Resistance of the IGBT when it is turned on.
Junction Temperature (Tj)	150	°C	Maximum temperature allowed at the IGBT junction.

⇒Choosing IR2103 DIP8 Half-Bridge Driver with following reasons:

The (R2103 is an integrated half-bridge driver designed for driving IGBTs and MOSFETs in motor control applications.

Table 4. *Parameter of IR2103*

Property	Value	Unit	Description
Supply Voltage (VCC)	7 ~ 25	V	Operating voltage range
Output Current (Peak)	1	A	Maximum peak output current
Output Voltage (High)	VCC - 1.5	V	High-level output voltage
Output Voltage (Low)	0.3	V	Low-level output voltage
Output Pulse Width (Typical)	50	ns	Typical output pulse width
Dead Time (Typical)	500	ns	Typical dead time between outputs
Short Circuit Protection	Yes		Protects against short circuits
Undervoltage Lockout	Yes		Prevents operation below VCC(UVLO)
Operating Temperature Range	-40 ~ 85	°C	Ambient temperature range

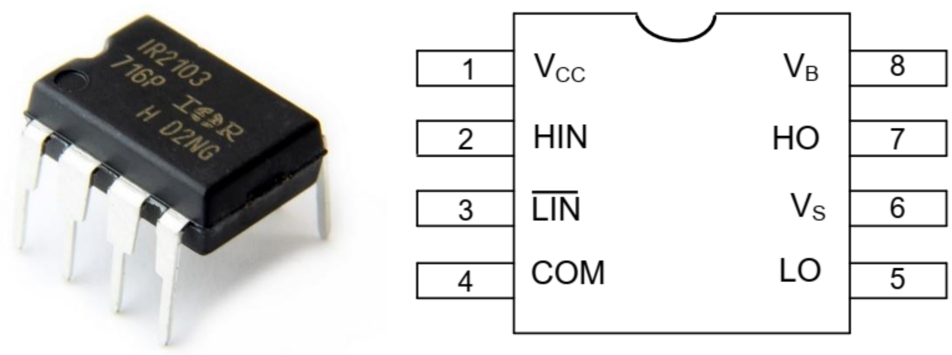

Figure 19. *IR2103 and Pin Diagram*

3.3.4. LC Output Filter

❖ Inductor Design:

With $\Delta V = 20\%\, V_{out,rms}$, so:

$\Rightarrow \Delta\, V = 20\% * V_{out,rms} = 20\% * \frac{12}{\sqrt{3}} = 1{,}39(V)$

$\Rightarrow X_{ls} = \frac{V_{ls}}{I_{out,rms}} = \frac{1.39}{2} = 0{,}695$

$\Rightarrow L_S = \frac{X_{ls}}{w} = \frac{0{,}695}{2\pi*50} = 2{,}2\ (mH)$

$\Rightarrow \Delta I_{V,max} = \frac{V_{in}*T_S}{2L_S} = \frac{21*0{,}5*10^{-4}}{2*2{,}2*10^{-3}} = 0{,}24(A)$ → Sastify the condition above.

⇒ Choose $L = 3.3\ mH$

❖ Capacitor Design:

$$w_{LC} = \frac{1}{\sqrt{L_s * C}} = 0{,}1 * w_s = 1000\pi\ (\frac{rad}{s})$$

$\Rightarrow C = \frac{1}{L_S * w_{LC}{}^2} = \frac{1}{2{,}2*10^{-3}*(1000\pi)^2} = 46{,}24(\mu F)\backslash$

⇒ Choose $C = 47uF$

3.3.5. Measurement Devices

❖ Current Sensor: ***Module ACS712-5A (Module ACS712-05B)***

Table 5. Properties of ACS712

Property	Value	Unit	Description
Current Range	5A, 20A, or 30A (model dependent)	A	Maximum measurable current
Sensitivity	185 mV/A, 100 mV/A, or 66 mV/A (model dependent)	mV/A	Output voltage change per unit of current
Output Voltage Range	-Vcc to +Vcc	V	Output voltage swing
Supply Voltage (Vcc)	4.5 - 5.5	V	Operating voltage range
Bandwidth	80 kHz	Hz	Frequency response
Accuracy	±1.5% (typical)	%	Measurement accuracy
Temperature Drift	±300 ppm/°C	ppm/°C	Sensitivity change with temperature

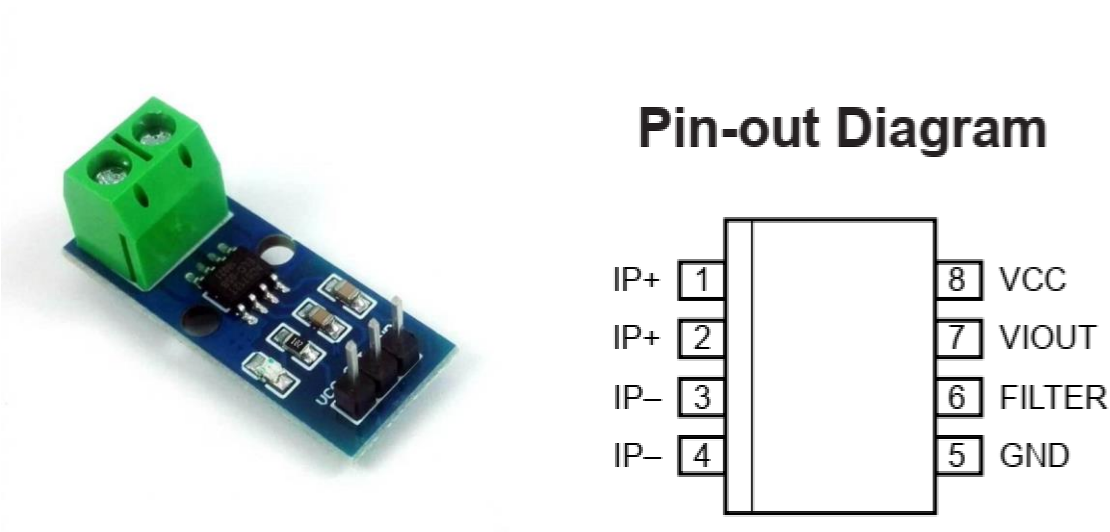

Figure 20. *ACS712 and Pin-out Diagram*

❖ Voltage Sensor: ***ZMPT101B***

Table 6. Properties of ZMPT101B

Property	Value	Unit	Description
Voltage Ratio	2000:1		Transformation ratio between input and output voltage
Accuracy	0.1%		Measurement accuracy
Frequency Range	50-400 Hz	Hz	Operating frequency range
Input Voltage	0-250 V AC	V AC	Maximum measurable voltage
Output Voltage	0-125 mV AC	mV AC	Output voltage corresponding to full-scale input
Operating Temperature Range	-40 to 85 °C	°C	Ambient temperature range for operation

Table 7. Pins of ZMPT101B

Pin Number	Pin Name	Description
1	Vout	Output signal pin, providing the scaled-down AC voltage (typically 0-125mV)
2	GND	Ground connection for the transformer
3	Vout (NC)	Not connected (no internal connection)
4	Vin	Input voltage terminal for the primary side of the transformer (connect to the AC voltage to be measured)
5	Vin (NC)	Not connected (no internal connection)

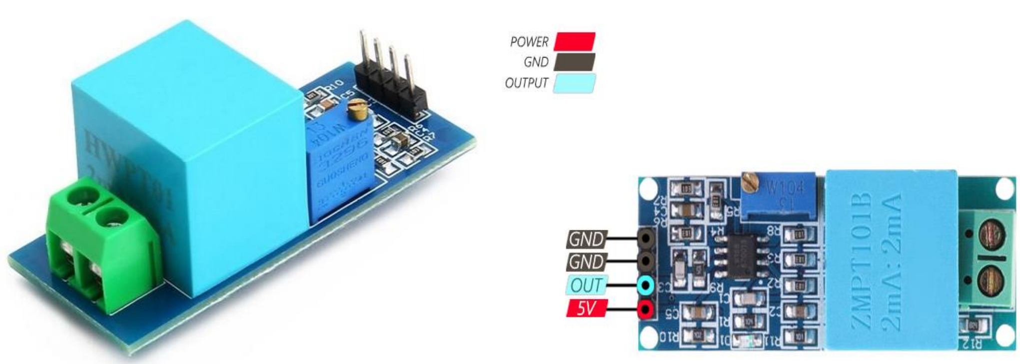

Figure 21. ZMPT101B and Pin-out Diagram

3.3.6. Microcontroller

With the simple construct and connection, so we choose kit Adruino Leonardo. The Arduino Leonardo is a microcontroller board based on the ATmega32u4. It has 20 digital input/output pins (of which 7 can be used as PWM outputs and 12 as analog inputs), a 16 MHz crystal oscillator, a micro USB connection, a power jack, an ICSP header, and a reset button. It contains everything needed to support the microcontroller; simply connect it to a computer with a USB cable or power it with a AC-to-DC adapter or battery to get started.

Table 8. *Parameter of Arduino Leonardo*

Property	Description	Unit
Microcontroller	Atmega32u4	
Operating Voltage	3.3V	
Input Voltage (recommended)	7-12V	V
Digital I/O Pins	14 (of which 12 provide PWM output)	
Analog Input Pins	7	
DC Current per I/O Pin	20 mA	mA
Flash Memory	32 KB (of which 4 KB used by bootloader)	KB
SRAM	2.5 KB	KB
EEPROM	1 KB	KB
Clock Speed	16 MHz	MHz
Length	68.6 mm	mm
Width	53.4 mm	mm
Weight	25 g	g
Unique Properties	* Built-in USB (native USB device) * Keyboard and mouse emulation * Native MIDI support	

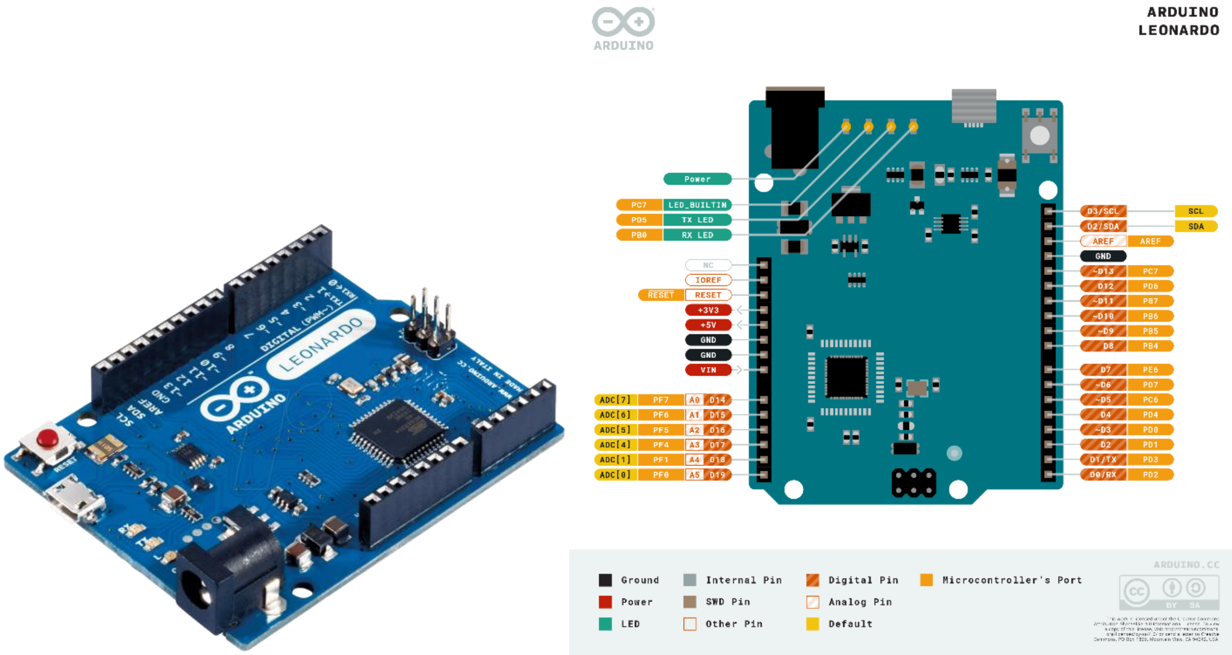

Figure 22. *Adruino Leonardo (Left) and the Pins Diagram (right)*

4.1. Simulation model

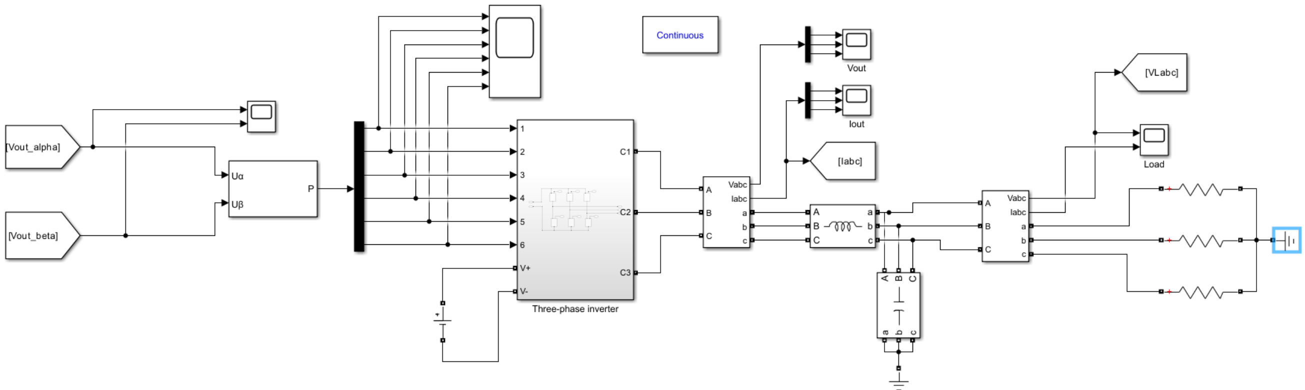

Figure 23. The block diagram of the power circuit in MATLAB SIMULINK

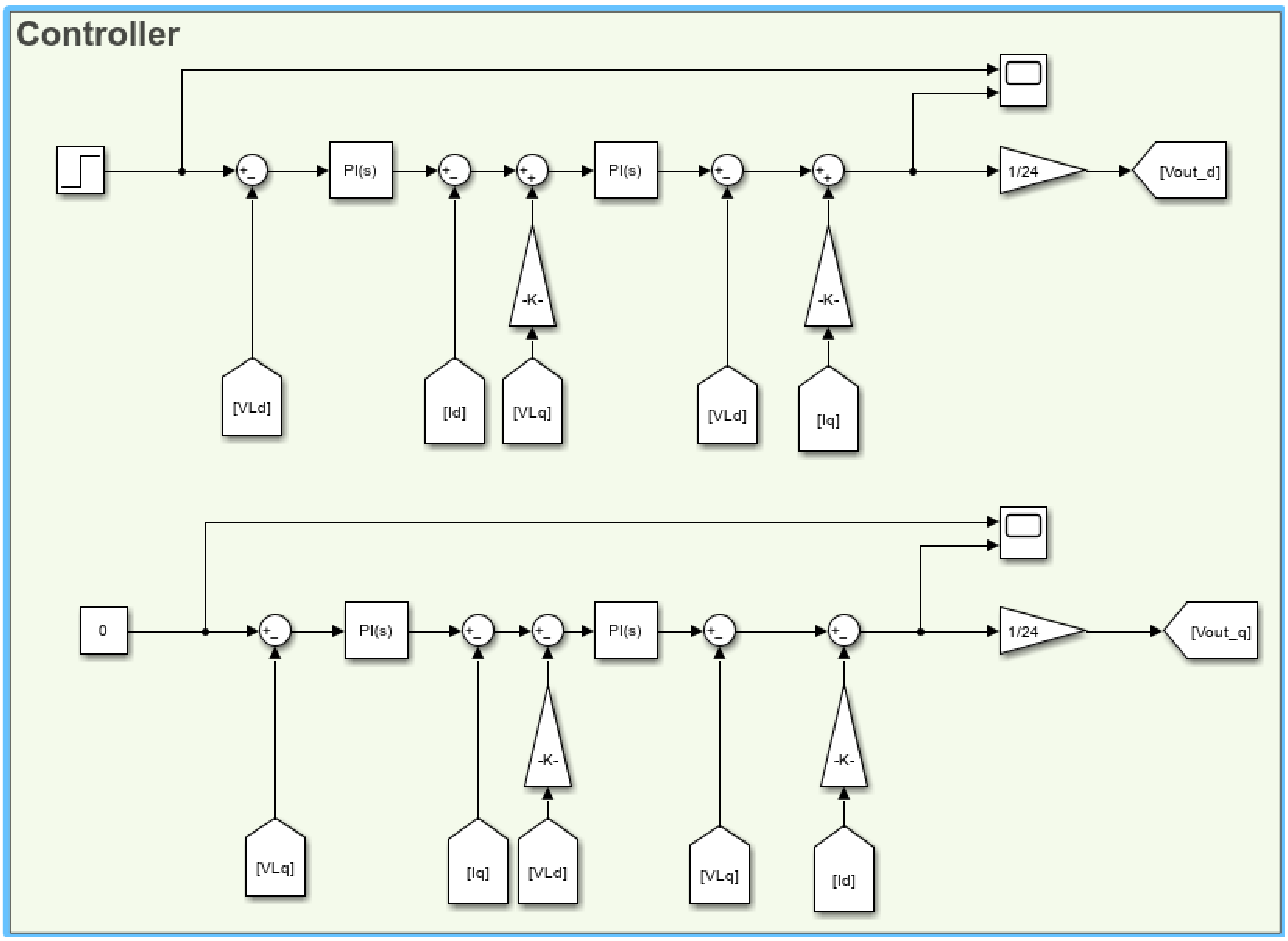

Figure 24. The outer voltage loop and inner current loop controller

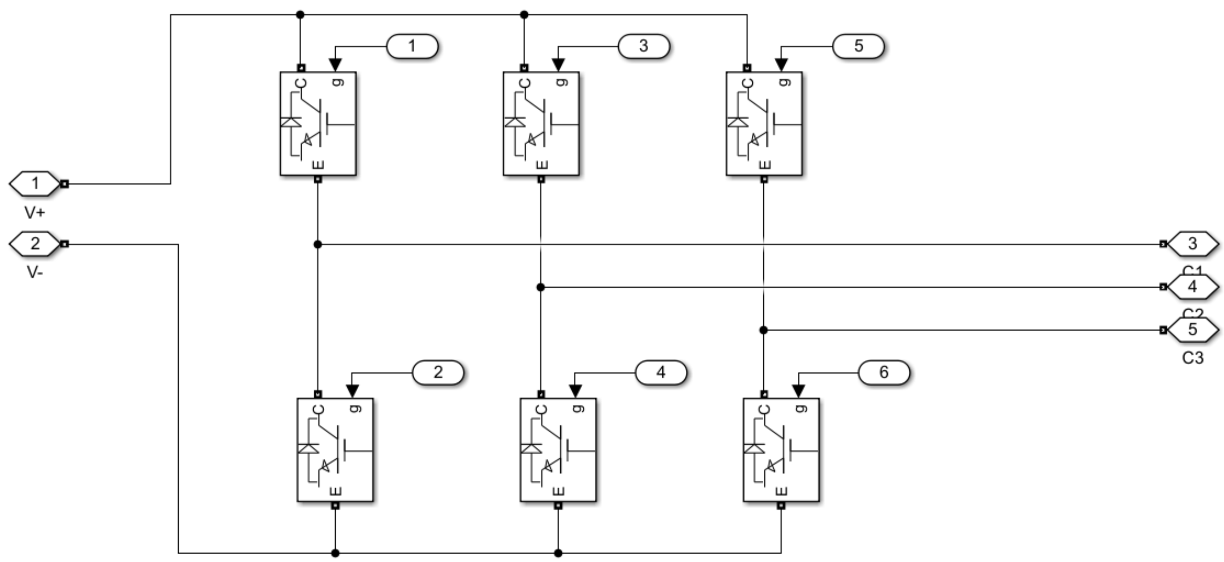

Figure 25. *The three phase inverter block diagram*

4.2. Space vector pulse width modulation model

The block's role is to convert the three-phase voltage in the Alpha/Beta frame into signals for MOSFETS drivers.

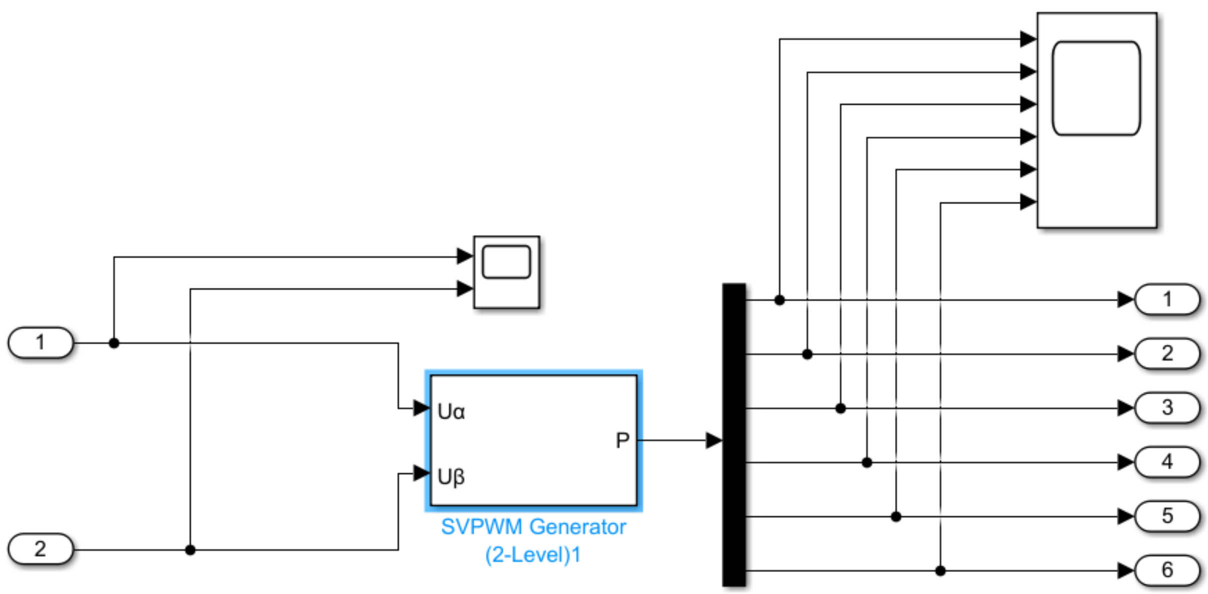

Figure 26. *SVPWM Block diagram*

Figure 27. *Gating signals (S1, S2, S3, S4, S5, S6) generated in Simulink.*

4.3. abc-to-dq transformation and dq-to-$\alpha\beta$ transformation models

4.3.1. abc-to-dq transformation model

The block's purpose is to convert the three-phase voltage in the rotating abc frame into the synchronous dq frame. Additionally, this block determines the instantaneous angle Theta (wt) of the fundamental frequency through Uq and uses it to execute the Park transform block. The transformation of the voltages from the abc frame into the dq frame is illustrated in the figures below.

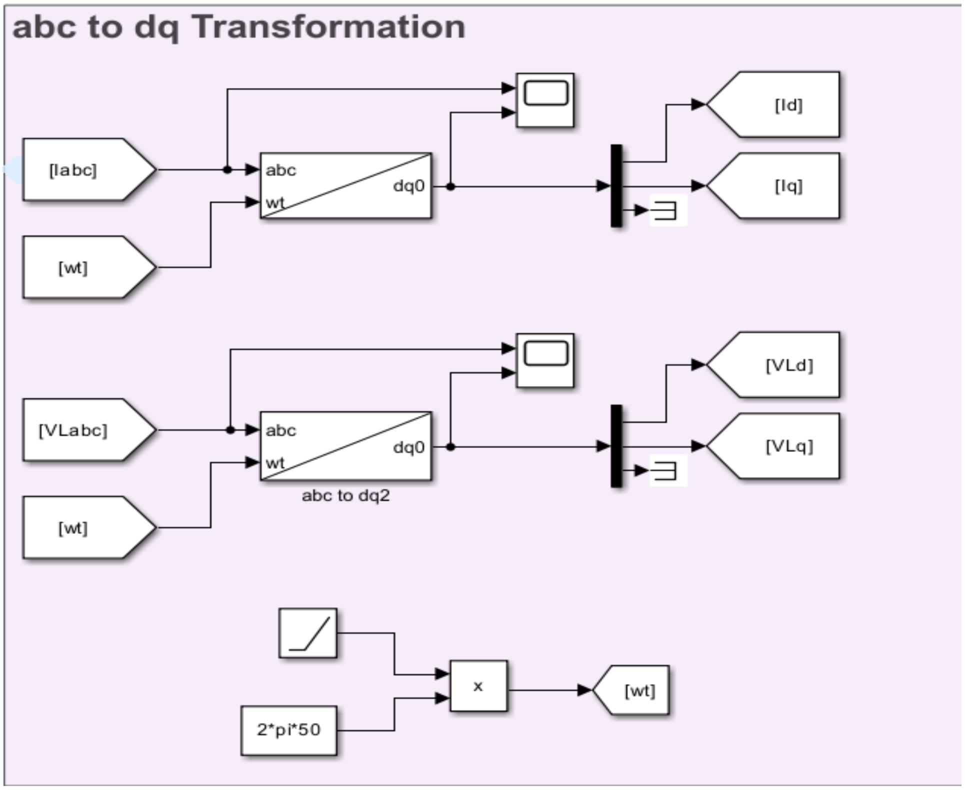

Figure 28. Transformation Reference three-phase voltage in abc frame to dq frame

4.3.2. dq-to- $\alpha\beta$ transformation model

The block's purpose is to convert the two-phase voltage in the synchronous dq frame into the stationary $\alpha\beta$ frame. The transformation of the voltages from the dq frame into the $\alpha\beta$ frame is illustrated in the figures below.

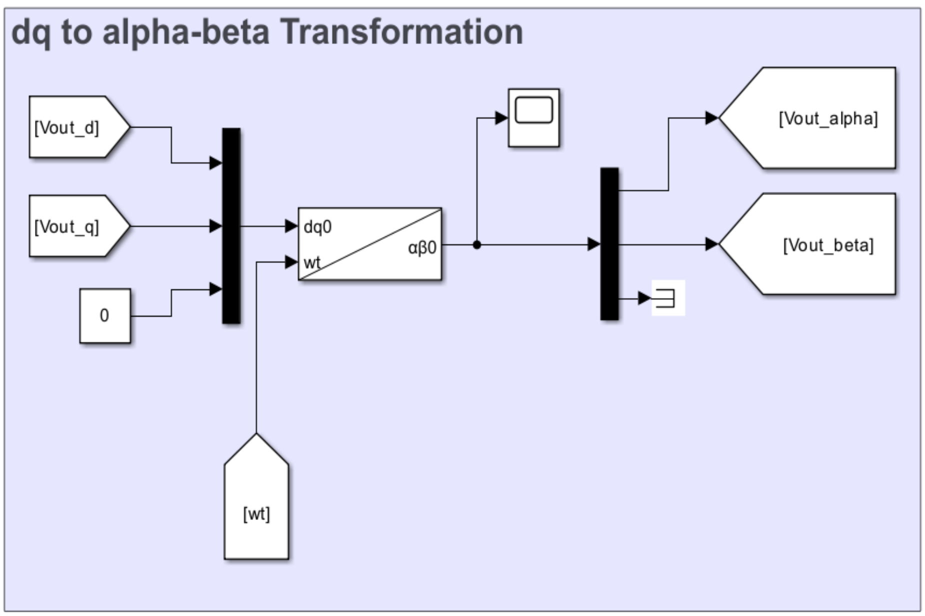

Figure 29. Transformation Reference three-phase voltage in dq frame to αβ frame

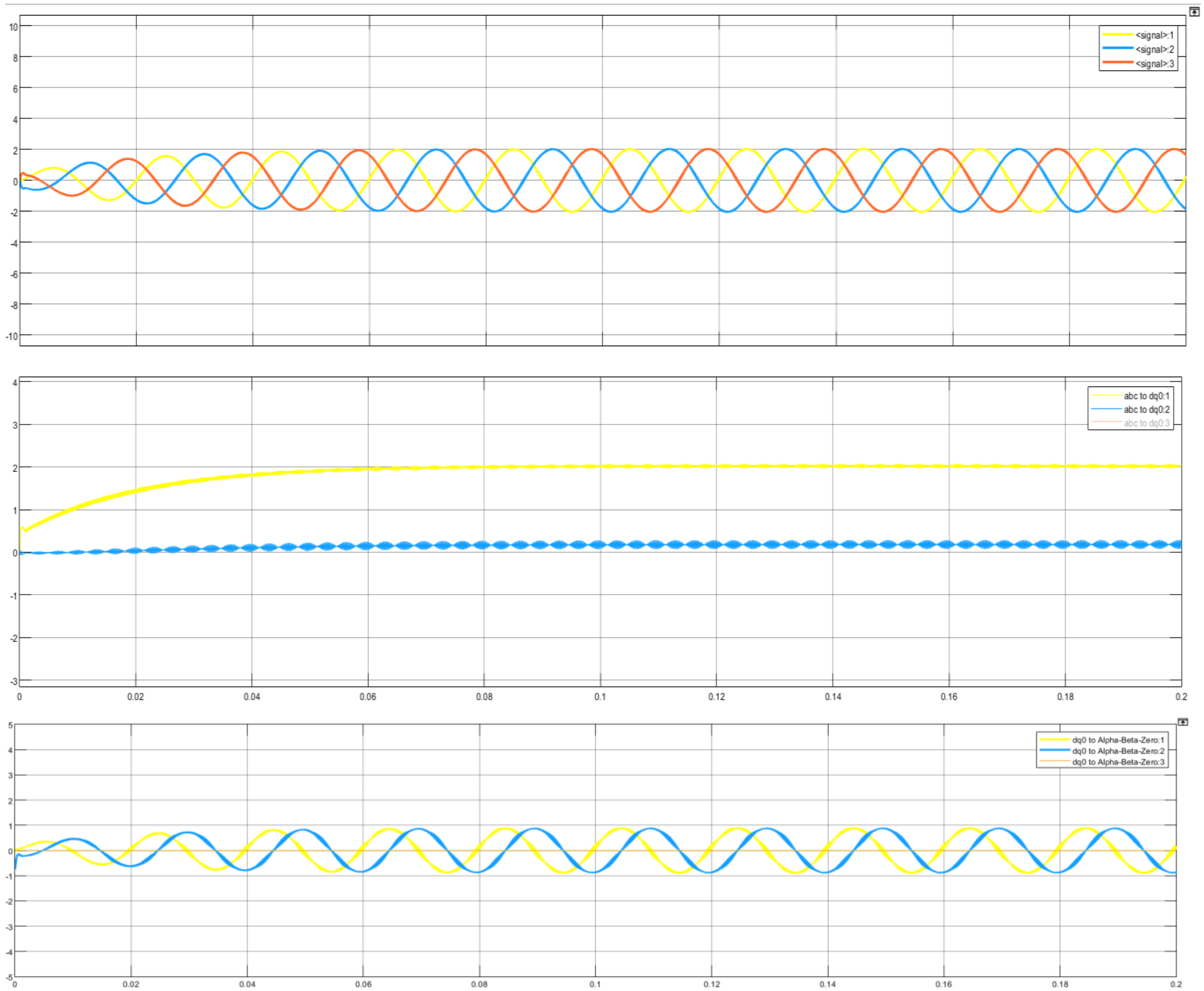

Figure 30. *Reference three-phase voltage in abc frame, dq frame, αβ frame*

4.4. Simulation result

The simulation is implemented in the loaded state with the specifications: $r_f = 6.6(m\Omega); L_f = 3.3\ (mH);\ ;\ C_f = 47\ (\mu F)$. Consider the load to be only resistor, a phase of load has $R = 6\ (\Omega)$. We obtain the three phase Voltage output and Current output as below:

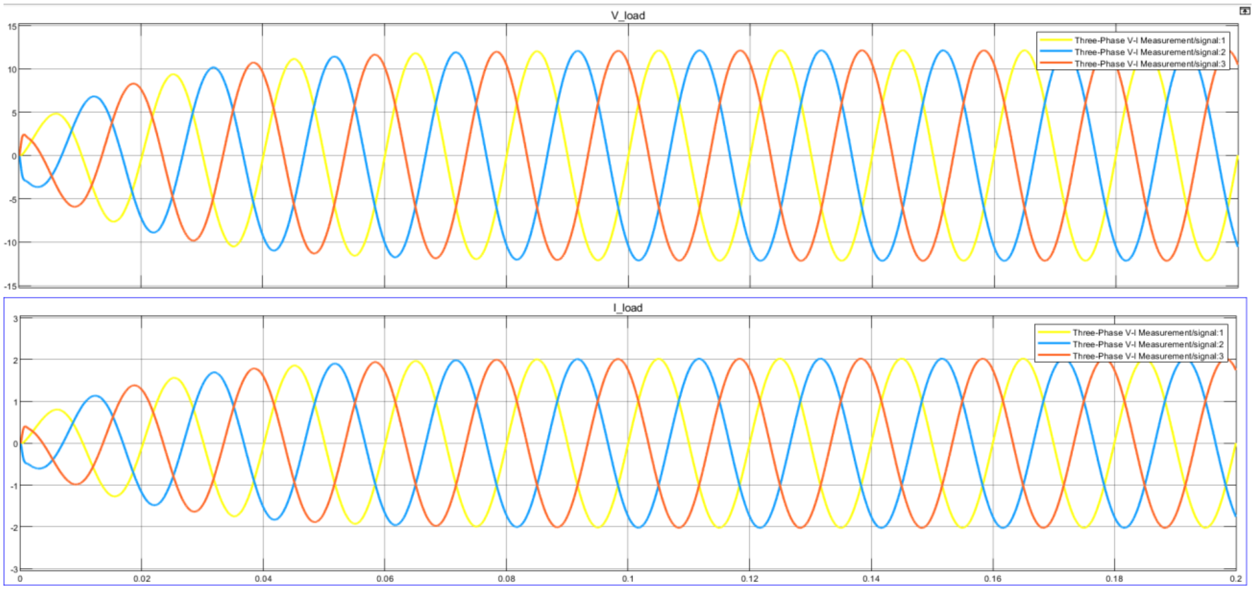

Figure 31. *Voltage output and Current ouput of the system*

CHAPTER 5. EXPERIMENTAL RESULT

Doing experiments in the laboratory, we found out that the voltage at output of load is approximately equal to 12V, with ripple about 10% because of wiring and error of measurement devices. The waveform of output voltage is not completely like the sine waveform in MATLAB Simulation.

This issue is attributed to the constraints associated with building the circuit on a breadboard, which can lead to inaccuracies in component values and energy losses that negatively impact the circuit's performance.

Moreover, if the output is incorrect, the data obtained from voltage and current sensors will also be incorrect, which can lead to inaccuracies in the control algorithm output and affect the PWM frequency used to control the MOSFETs.

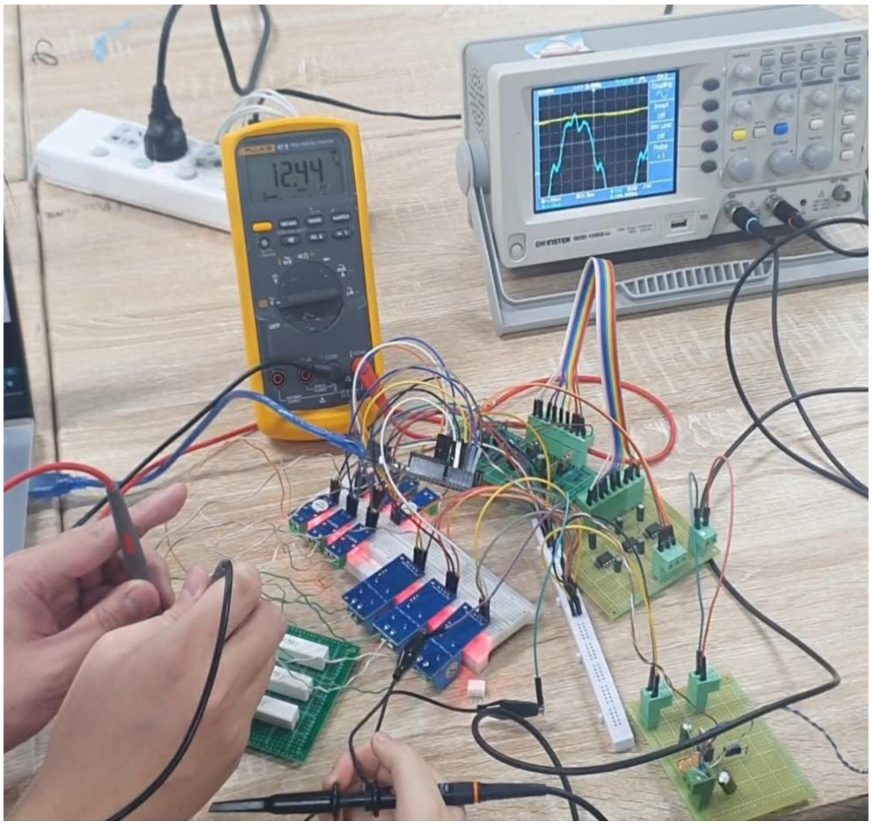

***Figure 32**. Voltage output of the system*

CONCLUSION

After one term 2023.1, the project for the “Digital Control” course, instructed by AsscProf. Vu Thi Thuy Nga, has come to the final result. Although the difficulty of reaching the desired goal for output voltage, the project provided us many knowledge including power electronics, control design and control theory, as well as embedded programming techniques.

Moving forward, we aim to expand the project by implementing our circuit on a Printed Circuit Board and experimenting with more professional microcontrollers such as Arduino. on the market . We extend our gratitude to AsscProf. Vu Thi Thuy Nga for her exceptional lectures and unwavering support throughout the semester’s project progression.